http://dx.doi.org/10.21577/0103-5053.20170179

J. Braz. Chem. Soc., Vol. 29, No. 3, 649-658, 2018.
Printed in Brazil - ©2018 Sociedade Brasileira de Química

Article

Novel Chemical Route for Deposition of Cu_2ZnSnS_4 Photovoltaic Absorbers

Gerardo Gordillo,[a] Raul A. Becerra[b] and Clara L. Calderón[a]*

[a]Departamento de Física and [b]Departamento de Química, Universidad Nacional de Colombia, 01111 Bogotá, Colombia

This work reports results of a study carried out to optimize the preparation conditions of Cu_2ZnSnS_4 (CZTS) thin films grown by sequential deposition of Cu_2SnS_3 (CTS) and ZnS layers, where the Cu_2SnS_3 compound was grown using a novel procedure consisting of simultaneous precipitation of Cu_2S and SnS_2 performed by diffusion membrane assisted chemical bath deposition (CBD) technique. The precipitation across the diffusion membranes allows achieving moderate control of release of metal ions into the work solution favoring the heterogeneous growth mainly through an ion-ion mechanism. Through a parameters study, conditions were found to grow Cu_2SnS_3 thin films which were used as precursors for the formation of Cu_2ZnSnS_4 films. The formation of CZTS thin films grown in the Cu_2ZnSnS_4 phase was verified through measurements of X-ray diffraction (XRD), X-ray photoelectron spectroscopy (XPS) and Raman spectroscopy. Solar cells with efficiencies of 4.9% were obtained using CZTS films prepared by membrane assisted CBD technique as absorber layer.

Keywords: Cu_2ZnSnS_4 thin films, diffusion membrane assisted CBD, XPS, Raman, solar cells

Introduction

The recent progress of the thin-film solar cell technology and its high efficiency of 22.6% for $Cu(In,Ga)Se_2$ based devices, demonstrate the viability of this technology as an option for large-scale power generation.[1] However, the limited availability of In and Ga as well as the high material expenses and heavy metal cadmium toxicity, brings some concern especially in view of the desired industrial mass production. Efforts are currently being made to fabricate solar cells with high conversion efficiency, low cost and based on abundant and pollution free materials like Cu_2ZnSnS_4 (CZTS) and $Cu_2ZnSnSe_4$ (CZTSSe).[2-4]

A variety of vacuum and solution based routes have been developed for the deposition CZTS thin films, the growth of single-phase CZTS films being the main barrier towards a reliable process. Despite this limitation, reasonably successful film deposition and device fabrication has been demonstrated for both vacuum and solution-based deposition approaches. Several groups have reported the fabrication of CZTS thin films using a variety of methods such as sulfurization, electrodeposition, radio-frequency (RF) sputtering and co-evaporation.[5-12] Mitzi and co-workers[13] achieved a 12.7% efficient $Cu_2ZnSn(Se,S)_4$ device fabricated from CZTSSe films prepared using a hydrazine-based pure solution approach and employing an In_2S_3/CdS double-emitter on CZTSSe absorbers upon annealing under optimized conditions.

In this work, we use a solution-based route to grow Cu_2ZnSnS_4 thin films, consisting in sequential deposition of Cu_2SnS_3 (CTS) and ZnS layers followed by annealing in sulfur ambient at 550 °C. The ZnS layer was deposited by the conventional chemical bath deposition (CBD) method and the compound Cu_2SnS_3 was grown in a one-step process using a novel chemical procedure which includes simultaneous precipitation of Cu_2S and SnS_2 performed by diffusion membrane assisted CBD technique to achieve a moderate control of release of metal ions into the work solution, details are given by Correa *et al.*[14] It is well known that in a CBD process, the controlled release of precursor ions to the work solution favors the ion by ion growth.[15] Therefore, we consider that a controlled release of ions achieved by the physical barrier provided by the diffusion membrane favors the growth ion by ion and prevents the cluster formation. This work presents a study of parameters that allowed to find conditions for the growth Cu_2SnS_3 films that were used successfully as a precursor layer in the formation of $Cu_2ZnSnSe_4$ thin films. The parameters studied included optimization of the control of the supply of ions by selecting adequately the porosity of the membranes. This aspect constitutes the main advantage of this method with respect to the

*e-mail: ggordillog@unal.edu.co

conventional CBD. Special emphasis was placed in optimizing the properties of the CZTS films with the intention of using them as absorber layer in solar cells.

Measurements of X-ray diffraction (XRD), X-ray photoelectron spectroscopy (XPS) and Raman spectroscopy confirmed the formation of the Cu_2SnS_3 compound as well as the Cu_2ZnSnS_4 compound. The applicability of the CZTS films grown using the procedure proposed in this work for photovoltaic devices has been demonstrated using them as absorber layer, in CZTS based solar cells.

Experimental

The CBD process has its basis on the controlled precipitation of some material onto the surface of a particular substrate. This precipitation could occur in homogeneous phase (i.e., in the solution), or heterogeneous phase (i.e., on the substrate), and the thin film formation takes place when the ionic product exceeds the solubility product.[16,17]

The growth of Cu_2SnS_3 films was performed on soda-lime glass or on Mo coated glass substrates following a new route developed in our laboratory, which involves simultaneous precipitation of Cu_2S and SnS_2 into a work solution where the substances react giving rise to the formation of the ternary compound. The co-precipitation of Cu_2S and SnS_2 was done using two spatially separated diffusion membranes of nitrocellulose with porosity of 0.45 μm. The first one contained a solution of $CuCl_2$ as Cu^{2+} ion source and the second one contained a $SnCl_2$ solution, which was complexed with sodium citrate ($Na_3C_3H_5O(COO)_3$) to form the $[SnH_nCit]^{(n-1)}$ complexes; these species diffuse through the membranes into a solution of sodium thiosulfate ($Na_2S_2O_3$) where HS^- ions are formed by hydrolysis. Sodium thiosulfate also acts as a reducing agent of Cu^{2+} ions to generate Cu^+ and as an oxidizing agent of the Sn^{2+} to obtain Sn^{4+}. The co-precipitation of Cu_2S and SnS_2 results in thin films of Cu_2SnS_3 that typically grow at a rate of 10 nm min^{-1}. The diffusion membranes are used to get a moderate control of release of metal ions into the work solution to favor heterogeneous growth mainly through an ion-ion mechanism.

The system implemented for the synthesis of Cu_2SnS_3 thin films includes a double-wall glass reactor, a magnetic and mechanical agitator of the work solution, membranes and substrate holders fabricated in Teflon and indirect heating of the work solution through a hot water flow that circulates between the walls of the reactor. This system also includes a pumping system and an electronic control proportional integral differential (PID) of the solution temperature. Details of the deposition system and of the possible reaction mechanism for the formation of the Cu_2SnS_3 compound are given by Correa *et al.*[14]

The preparation of Cu_2ZnSnS_4 films was achieved by sequential deposition of Cu_2SnS_3 and ZnS films followed by annealing at 550 °C in sulfur ambient. The synthesis of the Cu_2SnS_3 films was performed using the procedure described above and the ZnS films were deposited by conventional CBD method using a solution containing thiourea (CSN_2H_4) as source of HS^- ions, zinc chloride ($ZnCl_2.2H_2O$) as source of Zn^{2+} ions, sodium citrate ($Na_3C_6H_5O_7.2H_2O$) as complexing agent and ammonia (NH_3) for pH adjustment. The following chemical bath composition led to good results: [$ZnCl_2$], [thiourea] and [sodium citrate] with 30, 400 and 45 mM, respectively. During the deposition, the bath temperature was maintained at 80 °C and the solution pH around 10. The annealing was done using a furnace placed inside a chamber, which was previously evacuated up to reaching a vacuum of 5×10^{-5} mbar and then sulfur was supplied by evaporation at a temperature of 150 °C. Subsequently the CTS/ZnS system was heated at 550 °C. Cu_2ZnSnS_4 thin films were grown using a thickness ratio of CTS/ZnS of about 1.5. For solar cell fabrication, we used typically 1.5 μm thick CZTS films.

XPS analysis of the CZTS thin films was performed with an X-ray photoelectron spectrometer K-Alpha spectrometer (Thermo Scientific), using the AlKα radiation (1486.6 eV) for sample excitation. Further characterization involved X-ray diffraction on a Shimadzu-6000 diffractometer equipped with a CuKα source (wavelength λ = 1.54060 Å) and Raman spectroscopy on a Horiba-JobinYvon micro-Raman Spectrometer LabRamHR in back scattering configuration with a DPSS laser of 780 nm, 20 mW focused with a 50× objective. The film thickness was determined using a Veeco perfilometer, model Dektak 150 surface profiler.

Results and Discussion

Optimization of the synthesis parameters of the Cu_2SnS_3 compound

Initially a study was realized to determine the synthesis parameters that give place to the formation of single phase CTS films to be used later as a precursor in the synthesis of the Cu_2ZnSnS_4 compound. The study was initiated by obtaining the conditions to grow the binary compounds Cu_2S and SnS_2 using the diffusion membrane assisted CBD method, to be used later to obtain the Cu_2SnS_3 compound through co-precipitation of these. For that, an experimental design based on a matrix of twenty-five assays was employed, where the values of concentration of the metal precursor and synthesis temperature were varied in a wide range and the pH and concentration of

Table 1. Values of the synthesis parameters which led to the growth of thin films in the SnS_2 and Cu_2S phases

Synthesis parameter	Parameter values for the formation of SnS_2	Parameter values for the formation of Cu_2S
Concentration of $Na_2S_2O_3.5H_2O$ / mM	160	160
Concentration of $Na_3C_6H_5O_7.2H_2O$ / mM	180	
Concentration of $SnCl_2.2H_2O$ / mM	70	
Concentration of $CuCl_2.2H_2O$ / mM		15
pH	5.5	6
Temperature / °C	70	70

both sodium thiosulfate and complexing agent remained constant. Table 1 lists the parameter values that led to the formation of the Cu_2S and SnS_2 compounds.

In the second phase we studied the influence of the main parameters of synthesis on the growth rate of the CTS films, varying each one of these in a wide range and keeping constant the rest of parameters in the values listed in the Table 1. Figure 1 shows the influence of the main deposition parameters (growth temperature, $[Cu^{2+}]$, $[Sn^{2+}]$, pH, $[S_2O_3^{2-}]$) on the growth rate of the CTS films as well as the variation of the thickness of the CTS films as a function of the deposition time.

From the results of Figure 1 the following facts can be highlighted: (*i*) the growth rate of the CTS films increases significantly when the synthesis temperature is increased. This behavior seems to be related with the increase of both the probability that the molecules involved in the reaction exceed the activation energy of the process and the value of the constant of solubility product (K_{PS}) by increasing of the temperature, which favors the growth in heterogeneous phase. (*ii*) The curve of the growth rate of CTS films as a function of $[Cu^{2+}]$ shows that at concentrations less than 15 mM is given a linear growth, indicating that in this concentration range the CTS film grows predominantly in heterogeneous phase, possibly due to the fact that the concentration does not significantly exceed the product of solubility.[18] At concentrations greater than 15 mM a decrease of the growth rate is observed, apparently because in this concentration range, the co-precipitation of Cu_2S and SnS_2 occurs both in heterogeneous and homogeneous phase due to the high concentration of Cu^{2+} cations in the reaction.

On the other hand, the growth rate of CTS films as a function of $[Sn^{2+}]$ shows a behavior similar to that of the curve of growth rate *vs*. $[Cu^{2+}]$. In this case the linear growth occurs at concentrations less than 60 mM. At concentrations above 80 mM the growth rate decreases by increasing the concentration of Sn^{2+}, probably due to an excess of the metal precursor in solution which induces a strong growth in homogeneous phase. (*iii*) When the concentrations of $(S_2O_3^{2-})$ ions increases between 120 and

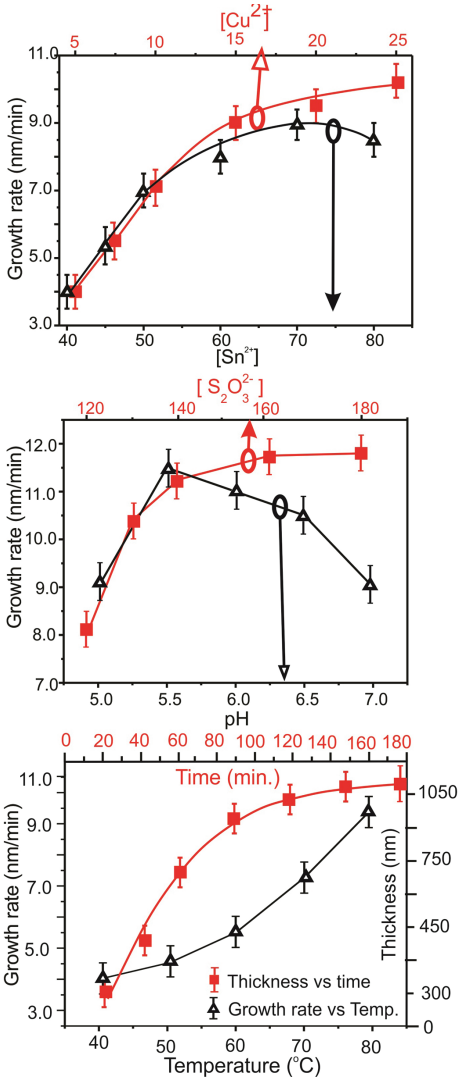

Figure 1. Variation of the growth rate of CTS films in dependence of: concentration of Cu^{2+}, concentration of Sn^{2+}, concentration of ion thiosulfate $(S_2O_3^{2-})$, synthesis temperature and pH (deposition time of 60 min). A curve of the variation of the thickness as a function of the deposition time is also displayed.

140 mM the growth rate of the CTS films increases very fast but at concentrations above 140 mM the growth rate tends to remain stable. This behavior could be explained by assuming that the increase in the concentration of $(S_2O_3^{2-})$

enhances the formation of the complexes with the cation Cu^{2+} giving rise to a strong increase in the growth rate of the CTS during the initial phase of formation. When the concentration of ($S_2O_3^{2-}$) ions becomes very high (> 140 mM), the growth rate of the CTS films increases very little due to the limited concentration of Cu^{2+} that participates in the reaction. (*iv*) The studies performed to evaluate the influence of the pH of the work solution on the growth rate of the CTS revealed that when the pH increases between 5 and 5.5, the growth rate of the CTS increases as a result of an increase in the value of the K_{PS} associated with a rapid speed of formation of the ion HS^-. However, at pH values greater than 5.5 the growth rate decreases, mainly due to a reduction in the speed of disproportionation of ion thiosulfate which causes a decrease in the concentration of ions HS^-.[19] (*v*) The curve of variation of the thickness of the CTS films in dependence of the deposition time shows two different regions during the growth process: an initial linear region (between 20 and 80 min) where the film thickness increases linearly and the final saturation region (after 120 min), which are typical of CBD processes. Before starting the linear growth region, there is a period of time of about 10 min (called induction time), during which the nucleation process is induced. Finally, during the saturation stage, the growth rate decreases significantly as consequence of a reduction of the reagent concentrations in the solution.

A study was additionally carried out with the purpose of finding the conditions for the growth of Cu_2SnS_3 films. For this, it was identified the phases present in CTS films deposited varying the concentration of Cu^{2+}, keeping constant the rest of synthesis parameters whose values correspond to those reported in Table 1. The identification of phases was carried out through measurements of XRD and Raman spectroscopy. Figure 2 shows typical XRD spectra corresponding to CTS films deposited varying the concentration of Cu^{2+} between 10 and 22 mM. After deposition, the CTS samples were annealed in sulfur ambient during 30 min at 550 ºC.

It is clear from the XRD spectra shown in Figure 2 that the samples prepared using a concentration of Cu^{2+} of 15 mM, exhibit reflections along the planes (112), (204) and (206) which correspond to the Cu_2SnS_3 phase (PDF file No. [00-027-0198]). It is also observed that the CTS sample deposited using a concentration of Cu^{2+} of 10 mM (Figure 2a) show in addition a reflection at 2θ = 32° which, according to the PDF file No. 00-014-0619, corresponds to the Sn_2S_3 phase. On the other hand, the diffractogram of the CTS film prepared at a concentration of Cu^{2+} between 18 and 22 mM (Figures 2c and 2d) exhibits reflections corresponding to the Cu_2SnS_3 phase and additionally a

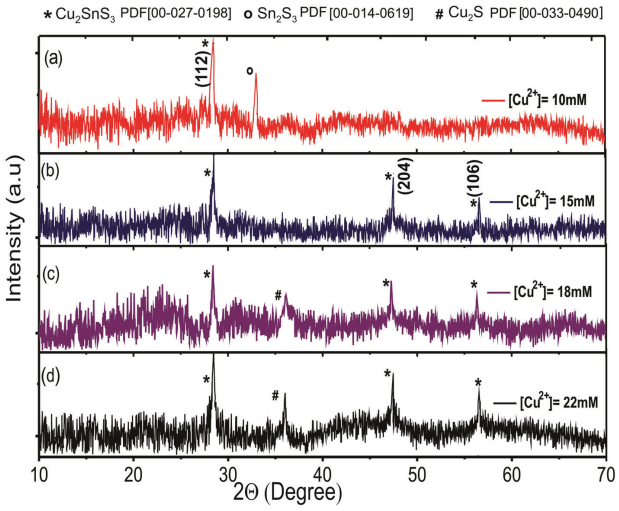

Figure 2. Diffractograms of CTS films synthesized by co-precipitation of Cu_2S and SnS_2, varying the concentration of the ion Cu^{2+}: (a) 10 mM; (b) 15 mM; (c) 18 mM; (d) 22 mM.

reflection in 2θ = 37° associated with presence of Cu_2S according to the PDF file No. [00-033-0490].

Figure 3 shows Raman spectra together with the fitting of the peaks with Lorentzian curves of the same four CTS films whose diffractograms are shown in Figure 2. It is observed that the CTS film prepared using a concentration of Cu^{2+} of 15 mM, exhibit Raman peaks at 289, 300, 335 and 353 cm^{-1} which have been assigned to the A' symmetry vibrational modes from the tetragonal Cu_2SnS_3 phase.[20-23] In addition, this sample exhibits a peak at 315 cm^{-1} which also has been assigned to the monoclinic Cu_2SnS_3 phase. However, other authors have observed peaks at 290, 314 and 352 cm^{-1} which were assigned to monoclinic Cu_2SnS_3.[24] These experimental data suggest the possibility of coexistence of both monoclinic and tetragonal phases.

The results of Figure 3 also reveal that CTS samples prepared at high concentration of Cu^{2+} (between 18 and 22 mM) present two additional Raman peaks in 264 and 475 cm^{-1} that have been assigned to the CuS phase.[25,26]

It is clear from the results presented in Figures 2 and 3 that the identification of the phases present in CTS films deposited by co-precipitation of Cu_2S and SnS_2, which were determined from XRD measurements, agree quite well with those obtained from Raman spectroscopy analysis. These results also allow concluding that tetragonal (or possibly mixture of tetragonal and monoclinic) Cu_2SnS_3 thin films can be grown by the diffusion membrane assisted CBD method using the values of synthesis parameter listed in Table 2.

The highest temperature that can be used to prepare CZTS films with adequate properties to be used in the fabrication of solar cells with improved conversion efficiency is 80 ºC, both for the layer of CTS and the layer of

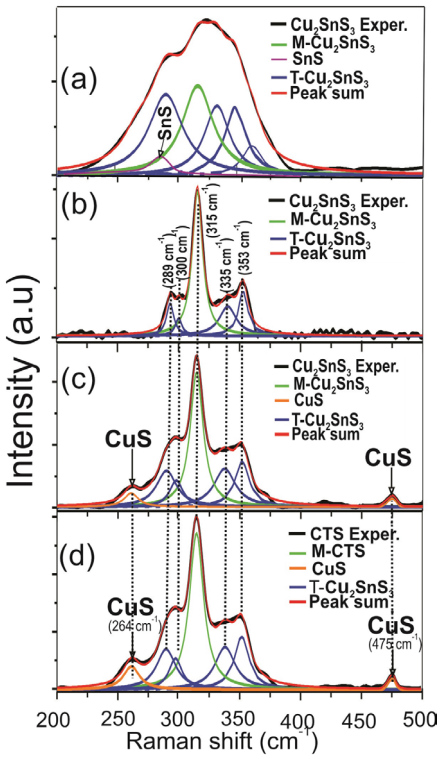

Figure 3. Raman spectra of CTS films synthesized by co-precipitation of Cu_2S and SnS_2, varying the concentration of the ion Cu^{2+}: (a) 10 mM; (b) 15 mM; (c) 18 mM; (d) 22 mM.

Table 2. Values of the synthesis parameters which led to the growth of Cu_2SnS_3 thin films using the diffusion membrane assisted CBD method

Synthesis parameter of Cu_2SnS_3 film	Parameter value
Concentration of $SnCl_2.2H_2O$ / mM	70
Concentration of $CuCl_2.H_2O$ / mM	15
Concentration of $Na_3C_6H_5O_7.H_2O$ / mM	170
Concentration of $Na_2S_2O_3.5H_2O$ / mM	160
pH	5.5
Temperature / °C	80

ZnS. Temperatures greater than 80 ºC favor a homogenous reaction between the reactants present in the precursor solutions of the CTS, resulting in a strong precipitation of these in the whole reactor and growth of CTS films with presence of secondary phases on the substrate. At temperatures lower than 80 ºC a heterogeneous reaction is given between the reactants present in the precursor solutions, but the growth rate of both the CTS and ZnS decreases strongly when it decreases below 80 ºC.

Optimization of the synthesis parameters of the Cu_2ZnSnS_4 compound

The preparation of Cu_2ZnSnS_4 thin films was achieved depositing sequentially the precursor compounds (CTS and ZnS) on glass substrates or on Mo coated glass substrates, following the sequence substrate/CTS/ZnS/CTS/ZnS, and subsequently subjecting them to annealing at 550 °C during 30 min under a partial pressure of sulfur. The CTS films were deposited using the parameters listed in Table 2 which resulted from the study of parameters described above and the ZnS films were deposited by conventional CBD method using the parameters reported in Experimental section.

To achieve good device efficiencies non-stoichiometric Cu-poor and Zn-rich kesterite films are required, with compositions typically in the range Cu/(Zn + Sn) = 0.7-0.9 and Zn/Sn = 1.1-1.4.[27,28] This is likely related to minimization of the formation of secondary phases as well as of defects affecting the optoelectronic properties of the layers. This desired adjustment was achieved following a simple procedure consisting in varying the thickness of the ZnS layer (d_{ZnS}) in a wide range, keeping constant the thickness of the CTS layer (d_{CTS}) around 400 nm. Very thin ZnS layers leads to Zn deficiency in the stoichiometric ratio of the CZTS compound, which leads to a mixture of Cu_2ZnSnS_4 and CTS, while very thick ZnS layers give rise to excess of Zn in the stoichiometric ratio of the compound CZTS which leads to a mixture of Cu_2ZnSnS_4 and ZnS. Considering that the thickness ratio of the layers of CTS and ZnS significantly affects the stoichiometry of the CZTS layer and therefore the performance of the devices, the method of preparation of the CZTS compound was improved to achieve better reproducibility in the formation of CZTS layers free of secondary phases. For this we used a methodology that includes the following: (*i*) preparation of the CTS layers using the parameters listed in Table 2 that guarantee a growth of the compound Cu_2SnS_3 free of secondary phases. (*ii*) Realization of studies to determine the thickness of the CTS layer as a function of the reaction time. (*iii*) The control of the ZnS thickness was optimized using a system developed at the Helmholtz Zentrum Berlin für Materialien und Energie (Berlin), for the heterogeneous material production pilot line, which allows monitoring the turbidity of the solution and the thickness of the ZnS prepared by CBD as a function of the reaction time.[29]

Figure 4A shows typical XRD spectra corresponding to CZTS films deposited on Mo coated glass substrate, varying the thickness of the ZnS films between 150 and 350 nm, keeping constant the thickness of the CTS layer around 400 nm. The influence of the concentration of Cu^{2+} on the phases present in CZTS films was also studied. Figure 4B shows XRD diffractograms corresponding to CZTS films prepared using a 250 nm thick ZnS layer and a 400 nm thick CTS layer deposited keeping the concentration of Sn^{2+} in 70 mM and varying the concentration of Cu^{2+} between 10 and 20 mM. After deposition, the CZTS samples were

annealed during 30 min at 550 °C inside a vacuum chamber under S-partial pressure.

The XRD patterns of the CZTS thin film exhibit in general Bragg peaks of (112), (220), (312) that according to the PDF file No. 00-026-0575 can be assigned to the diffraction lines of CZTS with a kesterite structure. However, the results of the Figure 4A are unexpected taking into account that the samples deposited using very thin layers of ZnS should include reflections corresponding to the CTS compound and the deposited using very thick layers of ZnS should include reflections corresponding to the ZnS. This behavior can be explained considering that the ZnS and the Cu_2SnS_3 that might be present in the analyzed samples have reflections in angles that coincide with those of the CZTS. Therefore in order to be able to identify with greater reliability the presence of secondary phases in the CZTS compound, we use additionally the technique of Raman spectroscopy.

It is also observed in Figure 4B that the samples of CZTS deposited with excess of Cu^{2+} ($[Cu^{2+}]$ = 20 mM) present an additional reflection (in 2θ = 37.1°) corresponding to the Cu_2S phase according to the PDF file No. [00-033-0490], while the layers of CZTS prepared with excess of Sn^{2+} ($[Cu^{2+}]$ = 10 mM) exhibit an additional reflection (in 2θ = 32.1°) corresponding the SnS phase according to the PDF file No. [00-053-0526] as expected.

Figure 5 shows Raman spectra together with the fitting of the peaks with Lorentzian curves of the same CZTS films whose diffractograms are shown in Figure 4. It is observed in Figure 5A that the CZTS film prepared using a 250 nm thick ZnS layer exhibit Raman peaks at 288, 337, 367 and 375 cm^{-1} which have been assigned to the tetragonal Cu_2ZnSnS_4 phase,[30-32] whereas the CZTS film prepared using a 150 nm thick ZnS layer exhibit two additional Raman peaks at 301 and 315 cm^{-1} which have been assigned to the tetragonal Cu_2SnS_3 phase and monoclinic Cu_2SnS_3 phase, respectively.[25] On the other hand, it is also observed in Figure 5A that the CZTS film prepared using a 350 nm thick ZnS layer exhibits Raman peaks associated just to the tetragonal Cu_2ZnSnS_4 phase, but the main peak located at 334-338 cm^{-1} is wider than the same peak of CZTS samples prepared using thinner layers of ZnS. The widening of this peak could be associated with a potential contribution of ZnS considering that presence of residual ZnS in CZTS films has been clearly identified at 348 cm^{-1}, by exciting the sample with a UV laser.[25] However, the presence of ZnS would lead to an asymmetric broadening of the peak towards higher wavenumbers. Therefore, the observed increase of the width is more likely related to a lower crystalline quality of this layer with a higher density of structural defects. This also agrees with the absence of the Raman mode A CZTS peak at 288 cm^{-1} in the spectrum from this sample.

From the results displayed in Figure 5B it is possible to visualize that CZTS films grown using as precursor a 400 nm thick Cu-poor CTS layer (Cu^{2+} concentration of 10 mM) exhibit Raman peaks at 307, 337, 367 and 375 cm^{-1} which have been assigned to the tetragonal Cu_2ZnSnS_4 phase and an additional peak at 296 cm^{-1},[30] which has been identified with tetragonal Cu_2SnS_3 phase and with an E symmetry mode of Cu_2ZnSnS_4.[32,33] It is also observed

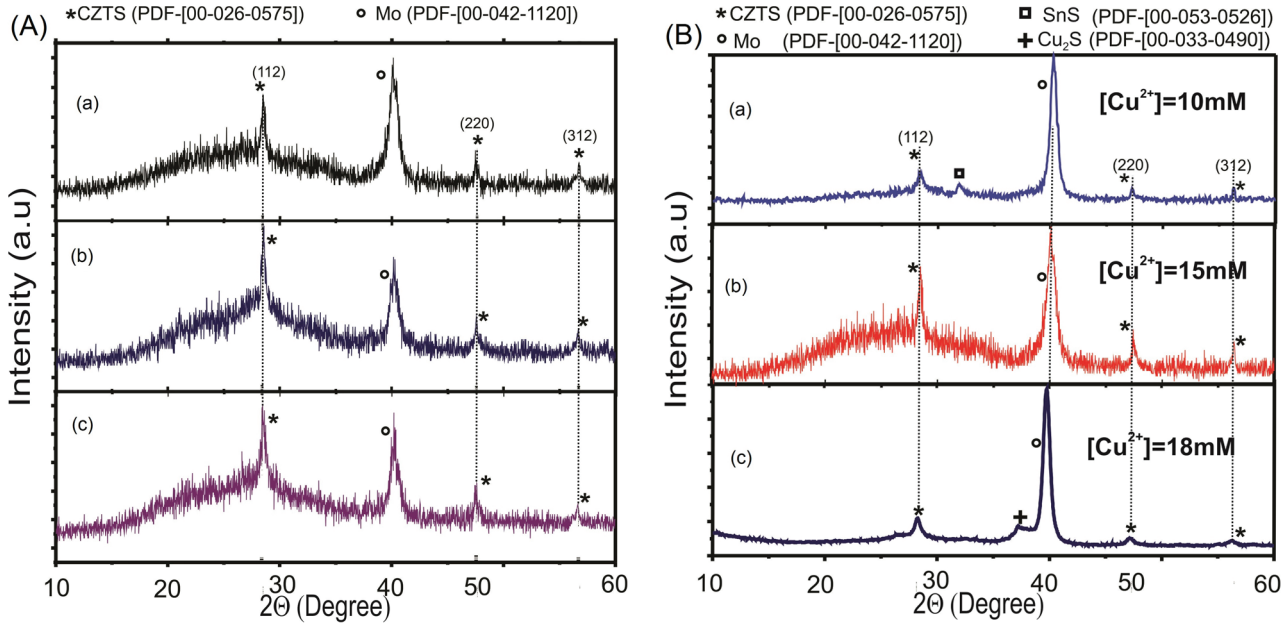

Figure 4. Diffractograms of CZTS films grown on Mo coated glass substrate prepared: (A) using a 400 nm thick CTS layer and ZnS films with different thicknesses: (a)150; (b) 250; (c) 350 nm and (B) using a 250 nm thick ZnS layer and a 400 nm thick CTS layer deposited keeping the concentration of Sn^{2+} in 70 mM and varying the concentration of Cu^{2+}: (a) 10; (b) 15; (c) 20 mM.

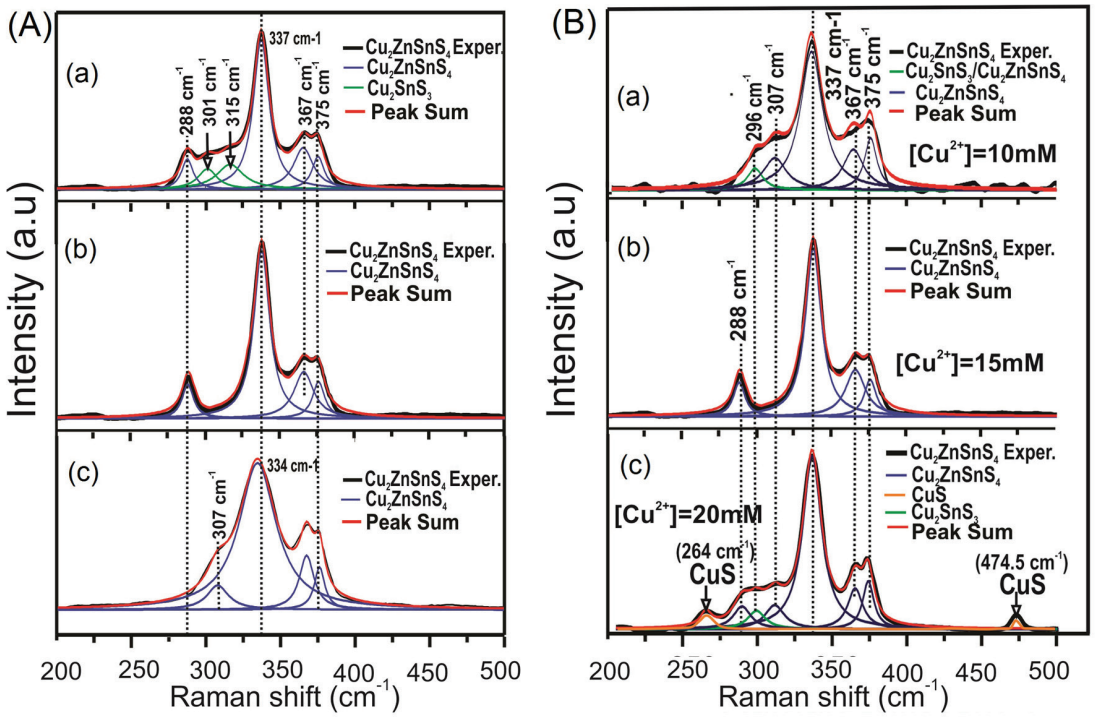

Figure 5. Raman spectra of CZTS films deposited: (A) using a 400 nm thick CTS layer ([Cu^{2+}] = 15 mM) and ZnS films with different thicknesses: (a) 150; (b) 250; (c) 350 nm; (B) using a 250 nm thick ZnS layer and a 400 nm thick CTS layer deposited keeping the concentration of Sn^{2+} in 70 mM and varying the concentration of Cu^{2+}: (a) 10; (b) 15; (c) 20 mM.

in Figure 5B that CZTS films grown using as precursor a 400 nm thick Cu-rich CTS layer (Cu^{2+} concentration of 20 mM) exhibit the same Raman peaks observed in the Cu-poor CZTS layer and two additional peaks at 264 and 474.5 cm^{-1}, associated to the CuS phase.[25,26]

XPS analysis

The oxidation states of a typical 0.65 μm thick CZTS film were determined through XPS measurements. Figure 6 displays the XPS survey spectrum and the high-resolution core level spectra corresponding to Cu 2p, Zn 2p, Sn 3d and S 2p regions of a typical 0.65 μm thick CZTS film. The S 2p core level spectrum exhibit peaks S $2p_{3/2}$ and S $2p_{1/2}$ with binding energies at 161.9 and 162.8 eV, consistent with the 160-164 eV range expected for S in sulfide phases.[34,35] The Sn $3d_{5/2}$ and Sn $3d_{3/2}$ peaks shown in Figure 6 are present at 486.4 and 494.5 eV, which confirms that Sn is in the +4 oxidation state.[34,35] The Cu 2p core level spectrum exhibit binding energies for the Cu $2p_{3/2}$ and Cu $2p_{1/2}$ peaks at 932.8 and 952.3 eV, respectively, and a peak splitting of 19.5 eV, enabling the conclusion that copper is in the +1 oxidation state and indicating the formation of copper(I).[31] Peaks Zn $2p_{3/2}$ and Zn $2p_{1/2}$ visible at binding energies of 1021.8 and 1044.6 eV with a peak separation of 22.8 eV suggest the presence of zinc(II).[34,35] The results obtained from the XPS analysis indicate that the oxidation states of the CZTS films prepared by the method proposed in this work correspond to the Cu_2ZnSnS_4 phase.

The results obtained in this work from XRD, XPS and Raman spectroscopy studies allow concluding that the route proposed in this paper is suitable for synthesizing thin films of Cu_2ZnSnS_4 using the parameters reported in Tables 1 and 2 and the procedure described above.

Performance of Mo/Cu_2ZnSnS_4/ZnS/i-ZnO/n^+-ZnO solar cells

The applicability of the CZTS films grown using the route proposed in this work for photovoltaic device fabrication was verified using them as absorber layer, in CZTS based solar cells. For that, solar cells with structure Mo/Cu_2ZnSnS_4/ZnS/i-ZnO/n^+-ZnO were fabricated and the current-voltage (J-V) characteristic was measured under AM 1.5 irradiance (100 mW cm^{-2}). Typically, the cells were fabricated using a 1.5 μm thick CZTS film, a 60 nm thick ZnS buffer layer deposited by CBD, a 30 nm thick i-ZnO layer and a 0.8 μm thick n^+-ZnO layer. The i-ZnO and n^+-ZnO layers were deposited *in situ* by reactive evaporation (details are given by Oyola *et al.*[36]). In Figure 7a the J-V curve of the best solar cell is displayed, presenting η = 4.9% with open-circuit voltage (V_{OC}) = 508 mV, short-circuit current density (J_{SC}) = 17.1 mA cm^{-2}, fill factor (FF) = 0.57. The active area of this device was 1.0 cm^2.

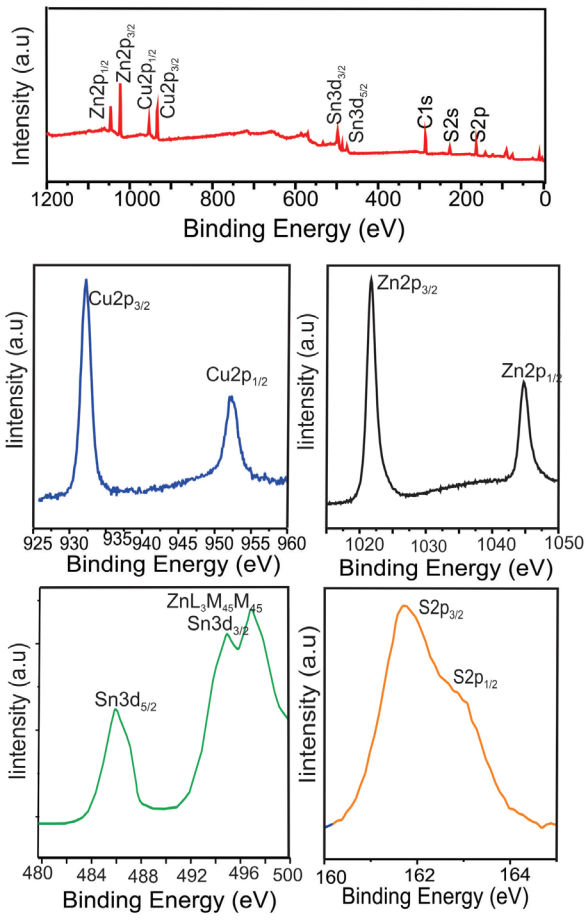

Figure 6. XPS Survey spectrum and high resolution scans of S 2p, Cu 2p, Sn 3d and Zn 2p peaks of a typical Cu_2ZnSnS_4 film.

Table 3 presents device characteristics of five solar cells fabricated varying the $[Cu^{2+}]/[Sn^{2+}]$ ratio of the CTS layer keeping constant the relationship between the thickness of the CTS layer with respect to the thickness of the ZnS layer (d_{CTS}/d_{ZnS} ratio) in a value of 1.5 (Zn-rich) as well as the d_{CTS}/d_{ZnS} ratio keeping constant the $[Cu^{2+}]/[Sn^{2+}]$ ratio in a value of 0.21. The parameters listed in Table 3 were measured with different degree of accuracy in such a way that the errors in each of the parameters listed in Table 3 are the following: the d_{CTS}/d_{ZnS} ratio measured using a Veeco Dektak 150 surface profiler was around 8%, the $[Cu^{2+}]/[Sn^{2+}]$ ratio determined on the basis of measurements made during the preparation of the precursor solutions was around 3% and the parameter characterizing the solar cell performance (J_{SC}, V_{OC}, FF and η), determined from the J-V curves automatically measured using a software developed for that purpose, was about 1.5%.

From the data in Table 3, it is observed that the low efficiency of CZTS devices is mainly caused by poor FF and low short circuit current (J_{SC}). Considering that the FF depends on the diode quality factor β as well as on effects of both series and shunt resistances, the high values of the series resistance (which has relation with the $[Cu^{2+}]/[Sn^{2+}]$ ratio of the cells) could be one of the causes of the low value of FF. On the other hand, taking into account that the diode quality factor is affected by recombination through trap centers inside the depletion region,[37] it can be considered that additional losses of the FF are related with

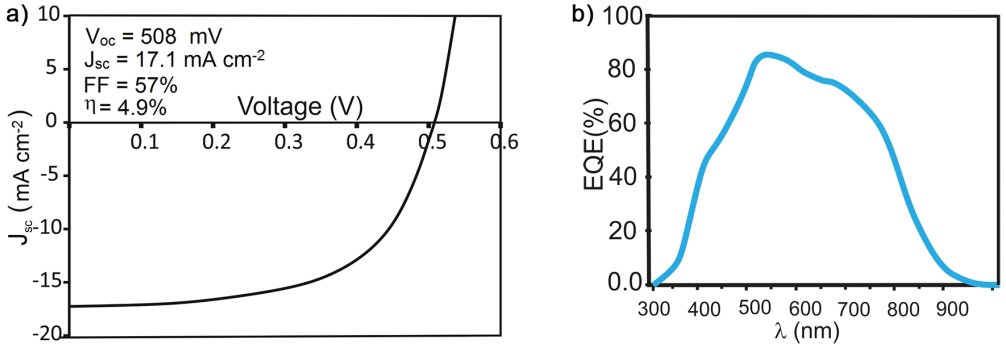

Figure 7. (a) J-V characteristic and (b) EQE of the best performance solar cell.

Table 3. Device characteristics of the performance of five CZTS based solar cells fabricated varying the $[Cu^{2+}]/[Sn^{2+}]$ ratio of the CTS layer and the d_{CTS}/d_{ZnS} ratio

d_{CTS}/d_{ZnS}	$[Cu^{2+}]/[Sn^{2+}]$	η / %	FF / %	V_{OC} / mV	J_{SC} / (mA cm^{-2})
1.5	0.14	3.4	48	482	15.1
1.5	0.21	4.9	57	508	17.1
1.5	0.25	4.7	57	490	16.8
1.5	0.31	4.3	53	470	17.3
2.2	0.21	4.2	55	480	15.9

d_{CTS}/d_{ZnS}: thickness of the CTS layer with respect to the thickness of the ZnS; η: efficiency; FF: fill factor; V_{OC}: open-circuit voltage; J_{SC}: short-circuit current density.

a high density of recombination centers in the depletion layer of the device. The low values of both V_{OC} and FF can be also attributed to the high conduction band offset at the CZTS/ZnS interface,[38,39] which can be reduced by decreasing the difference between the electronic affinities of the CZTS and ZnS. Improvement of the CZTS/ZnS interface could also be achieved reducing the density of states at the CZTS/ZnS interface, through a reduction in the density of acceptor impurities on the CZTS surface, which can be achieved by reducing the concentration of Cu at the end of the growth process of the CZTS layer.

The low value of J_{SC} of the cells fabricated in this work was evaluated analyzing the external quantum efficiency (EQE) shown in Figure 7b. The curve of the EQE witnesses an increase benefiting from the higher transparency of the window layer constituted by the system ZnS/i-ZnO/n^+-ZnO, due to the wider band gap of each of these layers (3.6 and 3.3 eV for ZnS and ZnO, respectively). However, the EQE decreases at long wavelength. This behavior may be attributed to a reduced minority carrier collection length in CZTS device. The collection length is approximately equal to the sum of the carrier diffusion length (L_d) and depletion width within the absorber part (W_d).

The depletion width in the absorber layer is determined by the electric field in the space charge region which is related to the carrier concentration in both absorber and buffer layer. The lower doping level characteristic of the ZnS used as buffer layer led to shorter depletion width within the absorber CZTS layer part, leading to an EQE decrease in long wavelength region.

On the other hand, the low values of J_{SC} suggest low collection of the photo-generated carriers which can be attributed to factors such as, short minority carrier diffusion length related with a high density of states associated with traps and centers of recombination induced in part by impurities present in the reagents used (99.5%). High recombination in states of interface may be another factor that contributes to the losses of the short circuit current.

The best efficiency obtained in this work (4.9%) is inferior to the highest efficiency reported currently for this type of cells fabricated by vacuum deposition process (9.5%).[39] However, bearing in mind that in this work preliminary results are presented, the performance of the cells could be increased by improving the crystallinity of the CZTS film by refining its growth process through a better control of the kinetics of growth and optimizing the parameters of synthesis. Taking into account that the diffusion membrane assisted CBD method allow optimizing the growth kinetics, we believe that this method is promising to prepare CZTS films for photovoltaic applications.

The performance of the devices could also be improved increasing the doping level of the buffer layer of ZnS, which can be achieved by doping it with indium (or aluminium) by adding a salt of In (or Al) to the precursor solution of zinc chloride. The increase of the doping level of ZnS gives rise to a widening of depletion width within the absorber CZTS layer part, which leads to an EQE increase in the long wavelength region and therefore to an increase of J_{SC}.

Conclusions

The conditions to obtain Cu_2ZnSnS_4 (CZTS) films prepared using a novel solution-based chemical route were optimized through an exhaustive study of the synthesis parameters. The growth of the CZTS samples was achieved by sequential deposition of Cu_2SnS_3 and ZnS thin films followed by annealing at 550 °C in an ambient of sulfur, where the Cu_2SnS_3 compound is prepared in one step process by simultaneous precipitation of Cu_2S and SnS_2 performed by diffusion membrane assisted CBD technique and the ZnS layer by conventional CBD methods.

Cu_2SnS_3 and ZnS films, which were used successfully as precursor layers for the formation of the Cu_2ZnSnS_4 compound, were achieved using the following chemical bath compositions: [$CuCl_2$], [$SnCl_2$], [$Na_2S_2O_3$] and [$Na_3C_6H_5O_7$] of 15, 70, 160 and 170 mM, respectively, bath temperature of 80 °C and pH around 5.5 for the preparation of Cu_2SnS_3 and [$ZnCl_2$], [$(SC(NH_2)_2)$] and [$(C_6H_5O_7^{3-})$] of 30, 400 and 45 mM, pH = 10 and bath temperature of 80 °C for the preparation of ZnS. XRD, XPS and Raman spectroscopy measurements confirmed the growth of Cu_2SnS_3 and Cu_2ZnSnS_4 films. The main advantage of the membrane assisted CBD method with respect to the conventional CBD, lies in the fact that the first one favors the heterogeneous growth, which contributes to prevent the formation of clusters, as a result of the physical barrier provided by the membrane.

The applicability for solar cells fabrication of the CZTS films prepared using the solution based chemical route proposed in this work was demonstrated. Efficiencies of 4.9% were achieved with solar cells fabricated with structure Mo/Cu_2ZnSnS_4/ZnS/i-ZnO/n^+-ZnO.

Acknowledgments

This work was supported by Colciencias (Contract No. 184/2016) and Universidad Nacional de Colombia, Sede Bogotá, Facultad de Ciencias, Bogotá DC, Colombia (Proy. 28135 supported by DIB). The authors would like to thank the Helmholtz Zentrum Berlin for its cooperation with the XPS measurements.

References

1. https://www.zsw-bw.de/fileadmin/user_upload/PDFs/Pressemitteilungen/2016/pr09-2016-ZSW-WorldRecordCIGS.pdf, accessed in October 2017.
2. Katagiri, H.; Jimbo, K.; Yamada, S.; Kamimura, T.; Maw, W. S.; Fukano, T.; Ito, T.; Motohiro, T.; *Appl. Phys. Express* **2008**, *1*, 041201.
3. Barkhouse, D. A. R.; Gunawan, O.; Gokmen, T.; Todorov, T. K.; Mitzi, D. B.; *Prog. Photovoltaics: Res. Appl.* **2012**, *20*, 6.
4. Todorov, T. K.; Tang, J.; Bag, S.; Gunawan, O.; Gokmen, T.; Zhu, Y.; Mitzi, D. B.; *Adv. Energy Mater.* **2013**, *3*, 34.
5. Araki, H.; Mikaduki, A.; Kubo, Y.; Sato, T.; Jimbo, K.; Maw, W. S.; Katagiri, H.; Yamazaki, M.; Oishi, K.; Takeuchi, A.; *Thin Solid Films* **2008**, *517*, 1457.
6. Yoo, H.; Kim, J. H.; *Thin Solid Films* **2010**, *518*, 6567.
7. Li, Y.; Yuan, T.; Jiang, L.; Liu, F.; Liu, Y.; Lai, Y.; *J. Mater. Sci.: Mater. Electron.* **2015**, *26*, 204.
8. Gougaud, C.; Rai, D.; Delbos, S.; Chassaing, E.; Lincot, D.; *J. Electrochem. Soc.* **2013**, *160*, D485.
9. Jimbo, K.; Kimura, R.; Kamimura, T.; Yamada, S.; Maw, W. S.; Araki, H.; Oishi, K.; Katagiri, H.; *Thin Solid Films* **2007**, *515*, 5997.
10. Liu, F.; Li, Y.; Zhang, K.; Wang, B.; Yan, C.; Lai, Y.; Zhang, Z.; Li, J.; Liu, Y.; *Sol. Energy Mater. Sol. Cells* **2010**, *94*, 2431.
11. Wang, K.; Gunawan, O.; Todorov, T.; Shin, B.; Chey, S. J.; Bojarczuk, N. A.; Mitzi, D.; Guha, S.; *Appl. Phys. Lett.* **2010**, *97*, 143508.
12. Shin, B.; Gunawan, O.; Zhu, Y.; Bojarczuk, N. A.; Che, S. J.; Guha, S.; *Prog. Photovoltaics: Res. Appl.* **2013**, *21*, 72.
13. Kim, J.; Hiroi, H.; Todorov, T. K.; Gunawan, O.; Kuwahara, M.; Gokmen, T.; Nair, D.; Hopstaken, M.; Shin, B.; Lee, Y. S.; Wang, W.; Sugimoto, H.; Mitzi, D. B.; *Adv. Mater.* **2014**, *26*, 7427.
14. Correa, J. M.; Becerra, R. A.; Ramírez, A. A.; Gordillo, G.; *EPJ Photovoltaics* **2016**, *7*, 70305.
15. Hodes, G.; *Chemical Solution Deposition of Semiconductor Films*; Marcel Dekker, Inc.: New York, USA, 2002.
16. Naghavi, N.; Abou-Ras, D.; Allsop, N.; Barreau, N.; Bucheler, S.; Ennaoui, A.; Fischer, C. H.; Guillen, C.; Hariskos, D.; Herrero, J.; Klenk, R.; Kushiya, K.; Lincot, D.; Menner, R.; Nakada, T.; Platzer-Björkman, C.; Spiering, S.; Tiwari, A. N.; Törndahl, T.; *Prog. Photovoltaics: Res. Appl.* **2010**, *18*, 411.
17. Gangopadhyay, U.; Kim, K.; Mangalaraj, D.; Yi, J.; *Appl. Surf. Sci.* **2004**, *230*, 364.
18. Pawar, S. M.; Pawar, B. S.; Kim, J. H.; Joo, O. S.; Lokhande, C. D.; *Curr. Appl. Phys.* **2011**, *11*, 117.
19. Pryor, W.; *J. Am. Chem. Soc.* **1960**, *82*, 4794.
20. Fernandes, P. A.; Salomé, P. M. P.; da Cunha, A. F.; *J. Phys. D: Appl. Phys.* **2010**, *43*, 215403.
21. Tanaka, T.; Yoshida, A.; Saiki, D.; Saito, K.; Guo, Q.; Nishio, M.; Yamaguchi, T.; *Thin Solid Films* **2010**, *518*, S29.
22. Altosaar, M.; Raudoja, J.; Timmo, K.; Danilson, M.; Grossberg, M.; Krustok, J.; Mellikov, E.; *Phys. Status Solidi A* **2008**, *205*, 167.
23. Lin, X.; Kavalakkatt, J.; Kornhuber, K.; Levcenko, S.; Lux-Steiner, M. Ch.; Ennaoui, A.; *Thin Solid Films* **2013**, *535*, 10.
24. Berg, D. M.; Djemour, R.; Gütay, L.; Siebentrit, S.; Dale, P. J.; Fontane, X.; Izquierdo, V.; Perez, A.; *Appl. Phys. Lett.* **2012**, *100*, 192103.
25. Sukarova, B. M.; Najdoski, M.; Grozdanov, I.; Chunnilall, C. J.; *J. Mol. Struct.* **1997**, *410*, 267.
26. Wang, S.-Y.; Wang, W.; Lu, Z.-H.; *Mater. Sci. Eng., B* **2003**, *B103*, 184.
27. Fairbrother, A.; Fourdrinier, L.; Fontané, X.; Izquierdo-Roca, V.; Dimitrievska, M.; Pérez-Rodríguez, A.; Saucedo, S.; *J. Phys. Chem. C* **2014**, *118*, 17291.
28. Fairbrother, A.; Dimitrievska, M.; Sanchez, Y.; Izquierdo, V.; Perez, A.; Saucedo, E.; *J. Mater. Chem. A* **2015**, *3*, 9451.
29. ASTM D1889-00: *Standard Test Method for Turbidity of Water,* West Conhohocken, Pennsylvania, USA, 2003.
30. Fernandes, P. A.; Salomé, P. M. P.; da Cunha, A. F.; *J. Alloys Compd.* **2011**, *509*, 7600.
31. Chalapathi, U.; Uthanna, S.; Sundara Raja, V.; *Bull. Mater. Sci.* **2017**, *40*, 887.
32. Guc, M.; Levcenko, S.; Bodnar, I. V.; Izquierdo, V.; Fontane, X.; Volkova, L. V.; Arushanov, E.; Perez, A.; *Sci. Rep.* **2016**, *6*, 19414.
33. Fernandes, P. A.; Salomé, P. M. P.; da Cunha, A. F.; *Phys. Status Solidi C* **2010**, *7*, 901.
34. Riha, S. C.; Parkinson, B. A.; Prieto, A. L.; *J. Am. Chem. Soc.* **2009**, *131*, 12054.
35. Xu, J.; Yang, X.; Yang, Q. D.; Wong, T. L.; Lee, C. S.; *J. Phys. Chem. C* **2012**, *116*, 19718.
36. Oyola, J. S.; Castro, J. M.; Gordillo, G.; *Sol. Energy Mater. Sol. Cells* **2012**, *102*, 137.
37. Mialhe, P.; Charles, J. P.; Khoury, A.; Bordure, G.; *J. Phys. D: Appl. Phys.* **1986**, *19*, 483.
38. Nagoya, A.; Asahi, R.; Kresse, G.; *J. Phys.: Condens. Matter* **2011**, *23*, 404203.
39. Sun, K.; Yan, C.; Liu, F.; Huang, J.; Zhou, F.; Stride, J. A; Green, M.; Hao, X.; *Adv. Energy Mater.* **2016**, *6*, 1600046.

Submitted: May 25, 2017
Published online: October 9, 2017